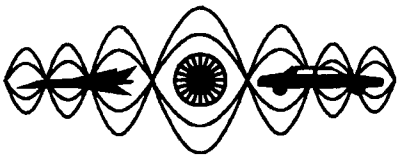

Tenth International Congress
on Sound and Vibration
7-10 July 2003 • Stockholm, Sweden

AN OVERVIEW OF RESEARCH ACTIVITY AT THE LAUNCH SYSTEMS TESTBED

Bruce Vu
NASA, John F. Kennedy Space Center, FL, USA
E-mail address: Bruce.T.Vu@nasa.gov

Max Kandula
Sierra Lobo, Inc. (USTDC), John F. Kennedy Space Center, FL, USA

Abstract

This paper summarizes the acoustic testing and analysis activities at the Launch System Testbed (LST) of Kennedy Space Center (KSC). A major goal is to develop passive methods of mitigation of sound from rocket exhaust jets with ducted systems devoid of traditional water injection. Current testing efforts are concerned with the launch-induced vibroacoustic behavior of scaled exhaust jets. Numerical simulations are also developed to study the sound propagation from supersonic jets in free air and through enclosed ducts. Scaling laws accounting for the effects of important parameters such as jet Mach number, jet velocity, and jet temperature on the far-field noise are investigated in order to deduce full-scale environment from small-scale tests [1].

INTRODUCTION

The LST evolved from vibroacoustics research and development conducted at KSC over the past two decades. The LST is located at the Launch Equipment Test Facility (LETF) in the KSC industrial complex. The Trajectory Simulation Mechanism (TSM) is a key component of the LST (Figure 1), designed specifically to accurately represent scaled testing of launch systems subjected to a moving rocket exhaust plume environment. In addition, the LST has developed in-house software for analyzing nonstationary random data and for predicting acoustic environments for launch pads.

ACOUSTIC TESTING

A schematic of TSM and related test setup is included in Figure 2. More details on the acoustic testing may be found in [2]. The TSM facility is outfitted with a chamber and a supersonic nozzle held in vertical position. The chamber is fed from pressurized gaseous nitrogen bottles (8000 psi) in conjunction with two pressure regulators in series. The nozzle (exit diameter of 1.0 inch) was scaled to represent a typical supersonic nozzle, capable of producing perfectly expanded flow at Mach 2.5. A rigid-walled duct with a traditional J-deflector is installed below the convergent-divergent nozzle (Figure 3). Measurements were made for both closed ducts and partially open ducts.

Data on chamber pressure, temperature, and pitot and static pressures at the NEP are recorded. Acoustic data are recorded after a steady-state condition is achieved. Acoustic measurements were made by an array of B&K microphones placed azimuthally at 22.5-degree increments. To measure far-field sound levels, the microphones were placed at an arc radius of 80 nozzle exit diameters from the nozzle exit plane (NEP).

Figure 4 shows a comparison of the overall sound pressure level (OASPL) for free jet with those of a jet passing through a closed duct, with the NEP located at different heights relative to the duct inlet. While there is axial symmetry of the OASPL for the free jet, there is considerable directivity of the OASPL in the presence of exhaust duct. For the nozzle-to-duct inlet distances of 5 inches and -1 inch (NEP inside the duct), the OASPL near the duct axis exceeds the value for the free jet case. When the NEP is held at 10 inches above the duct inlet, a reduction in OASPL of about 3 dB is achieved relative to the free jet case.

NUMERICAL SIMULATIONS

Prediction of Supersonic Jet Noise

The CFD/Kirchhoff analysis of an axisymmetric jet is based on the application of a Navier-Stokes CFD code for identifying the noise sources in the source-field and Kirchhoff surface integral for the propagation of sound radiation to the near-field and the far-field [3]. The Kirchhoff surface, enclosing the nonlinear source region, is chosen in a region where the linear wave equation is valid. By restricting the use of CFD methods to the near-field region for source identification, computational requirements are greatly reduced.

Figure 5a presents the contours of mean velocity and instantaneous sound pressure in the jet as computed by the CFD solution. The mean velocity contours show the extent of the potential core and the turbulent mixing layer. The pressure contours show the origination of Mach waves within the jet. From the OASPL contours in far-field as computed by the Kirchhoff integral, it is seen that the OASPL ranges from 80 dB to 130 dB in this region. The directivity of the Mach wave radiation (emission) is evident.

The variation of the OASPL in the streamwise direction at $z/r_j = 80$ is compared in Figure 5b with the measurements of Seiner et al. [4] for jet of Mach number 2 and a jet

exit temperature of 754 R (nozzle exit diameter of 3.6 inch). The predicted peak angle of emission of about 128 degrees is in good agreement with the data, which indicates a peak at 127 degrees. Also, the peak value of the OASPL is about 7 dB less than the measured value. There is an underprediction of the OASPL at the off-peak locations both upstream and downstream of the peak. By including azimuthal mode instability in a three-dimensional analysis, predictions of sound pressure levels could be improved.

Sound Propagation in a Duct With Rigid and Impedance Walls

Numerical experiments are carried out to study the propagation of plane acoustic waves in a two-dimensional duct with rigid, impedance, and flexible surfaces with and without mean flow [5]. A modified McComack's scheme is employed to solve the unsteady Euler equation. The boundary conditions are specified by a method of characteristics that represent the acoustic waves, the vorticity wave, and the entropy wave. In the far field, radiation boundary condition was used to simulate outgoing waves.

The directivity of acoustic wave propagating away from a duct (11 inches wide and 33 inches long) with zero mean flow is investigated. Figure 6a shows a comparison of pressure contour plots for the rigid surface case and the case with an impedance wall at the bottom and a plane wave frequency of 500 Hz. There are small differences between the two plots both inside and outside the duct. Figure. 6b shows the directivity pattern along a semi-circle of radius 2-feet centered at the exit of the duct. The use of the impedence surface results in slightly lowering the far field OASPL. The strongest effect is obtained when a flexible surface is used on the top wall. In this case the directivity pattern is asymmetric, and an increase of 7 dB is obtained at various points in the upper quadrant. Combining a flexible surface with an impedence wall slightly reduces the OASPL.

The variation of the overall sound pressure level over the top wall of the duct (2 inches wide and 33 inches long) with the downstream distance is shown on Figure 7. There is a significant reduction of the effect of the impedance wall on the OSPL. The decrease in OSPL over the length of the duct is reduced to about 20 dB from the 30 dB for the no-mean flow case. When a flexible surface is combined with an impedance wall, the reduction is even smaller (around 15 dB).

Unified Finite-Element Method (FEM) Program

Finite element is traditionally recognized by its versatility for handling complicated geometries at a relative ease. The objective is to develop an FEM solver for the Compressible Fluid Dynamics problems using the Mixed Explicit Implicit (MEI) method, then to incorporate the governing vibration and acoustic equations into the model. The second objective is to develop a user-friendly environment in which simulation programs and post processing of data can be carried out with relative ease. The preprocessor, solver and postprocessor will be accessible simultaneously (Figure 8). The main feature of this program is its user friendliness, in that the user will be able to access all input and output files in one unified environment.

ACOUSTIC SCALING

Proper care needs to be exercised in extending small-scale test data to full-scale application. In a recent paper [6], it has been demonstrated that the jet Mach number, rather than the ratio of jet velocity to ambient sound velocity, is the proper scaling parameter for correlating high-temperature jet noise. The effect of jet temperature is accounted for by Lighthill's suggestion through the changes in the density factor in the quadrupole field. Figure 9 shows the variation of predicted OASPL with the jet Mach number for a perfectly expanded jet for various values of the jet temperature. The OASPL is plotted relative to the value for jet Mach number of 1.0. The OASPL transitions from a u_j^8 dependence in subsonic flow to a u_j^3 dependence in highly supersonic flow. It is seen that at a given jet Mach number the OASPL increases with the jet temperature. These results are in general agreement with some of the available data.

HOT JET FACILITY DEVELOPMENT

As indicated, the effect of jet temperature on sound pressure level is significant; therefore, it is important to incorporate hot chamber conditions to provide a range of jet exhaust temperatures. LST is currently developing a new capability to include a hot air facility capable of producing high-temperature supersonic jets. The facility would greatly reduces the amount of testing and costs associated with full-scale rocket engine testing while providing valuable data on supersonic and hypersonic performance of new generation propulsion. The proposed hot jet facility includes a Sudden Expansion (SUE) propane burner.

CONCLUSION

The Launch Systems Testbed is a spaceport technology development capability available at the Kennedy Space Center. LST goals include reduction of launch-related costs and an increase in reliability, availability, and maintainability of launch structures, facilities, and equipment exposed to rocket launch environments. Current activities at the LST include but are not limited to subscale acoustic testing, numerical simulations, and acoustic scaling methodology. In addition, new capability is being added to include a hot jet facility, which is critical to the development of scaling and similarity laws for application to full scale.

ACKNOWLEDGEMENT

The authors thank Greg Moster and the Reusable Military Launch Systems (RMLS) team of Wright-Patterson Air Force Research Laboratory (AFRL) for continual support of the vibroacoustics research at KSC. The KSC engineering team that contributed to the testing efforts includes Wayne Crawford, Geoffrey Rowe, Jeffrey Crisafulli, Charles Baker, and Danielle Ford. Dr. Kader Frendi of University of Alabama in Huntsville provided

numerical study related to acoustic wave propagation through ducts with rigid, impedence and flexible surfaces. Dr. Amir Mobasher of Alabama A&M University collaborates with the LST in developing the finite-element techniques for solving rocket acoustics problems. The authors also express their appreciation to KSC management for their encouragement and interest in the research activities of the LST.

REFERENCES

1. Vu, B.T., Kandula, M., Margasahayam, R., and Ford, D., "Launch Systems Testbed: An Innovative Approach to Design of Future Space Structures," Space Technology and Application International Forums, Albuquerque, NM, Feb. 2-6, 2003.

2. Kandula, M., Margasahayam, R., and Vu, B., Sound Propagation From a Supersonic Jet Flowing Through a Rigid-Walled Duct With a J-Deflector, 10th International Congress on Sound and Vibration, July 7-10, 2003, Stockholm, Sweden.

3. Kandula, M., and Caimi, R., Simulation of Supersonic Jet Noise With OVERFLOW CFD Code and Kirchhoff Surface Integral, AIAA-2002-2602, 8th AIAA/CEAS Aeroacoustics Conference, Breckenridge, Colorado (2002).

4. Seiner, J.M., Ponton, M.K., Jansen, B.J., and Lagen, N.T., The Effects of Temperature on Supersonic Jet Noise Emission, AIAA 92-02-046, 1992.

5. Frendi, A., and Vu, B., On the Propagation of Plane Acoustic Waves in a Duct With Flexible and Impedence Walls, NASA TM-2203-211185, 2003.

6. Kandula, M., and Vu, B., On the Scaling Laws for Jet Noise in Subsonic and Supersonic Flow, AIAA-2003-3288, 9th AIAA/CEAS Aeroacoustics Conference, Hilton Head, South Carolina, May 12-14, 2003.

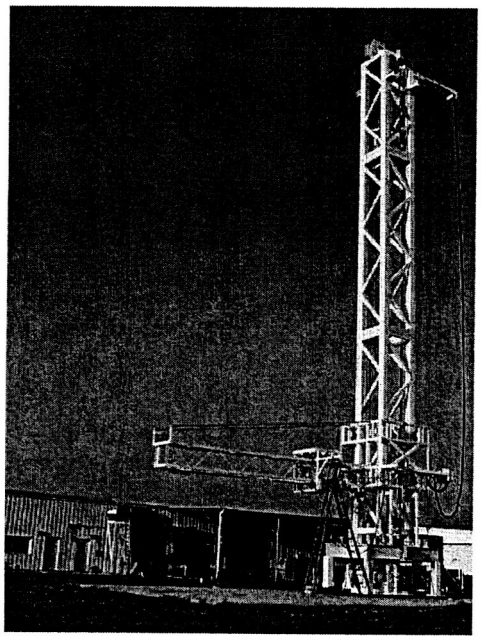

Figure 1. Trajectory simulation mechanism

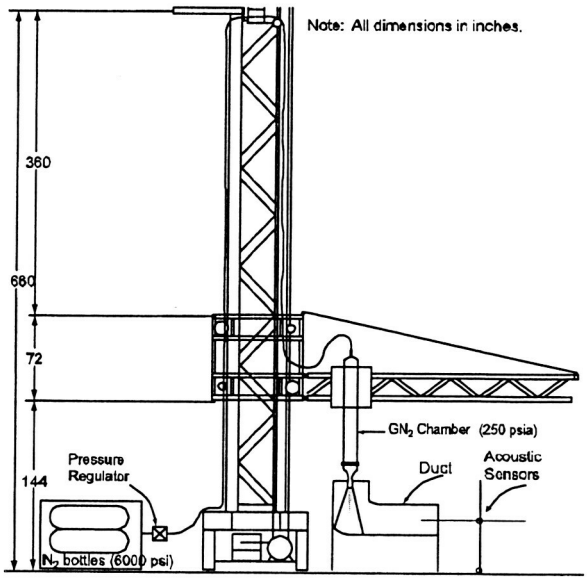

Figure 2. Overall test setup

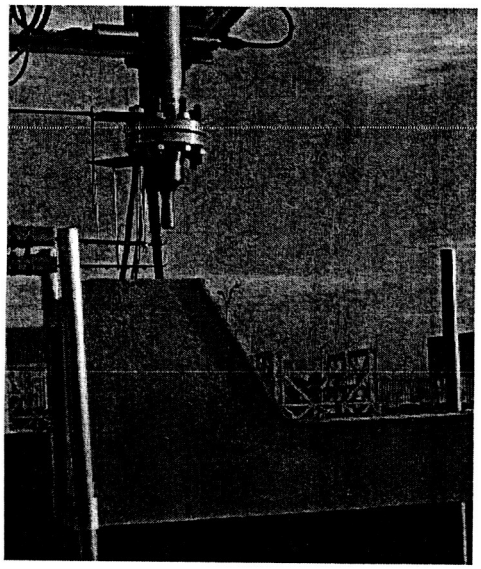

Figure 3. Nozzle/duct configuration

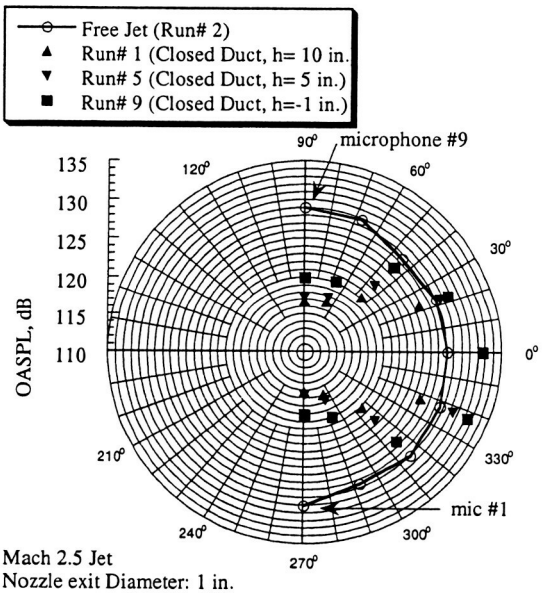

Figure 4. Comparison of OASPL for free jet and with a closed duct

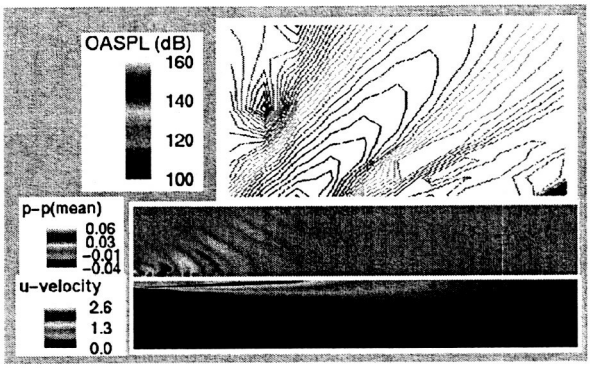

Figure 5a. Contours of OASPL Predicted From CFD/Kirchhoff Method

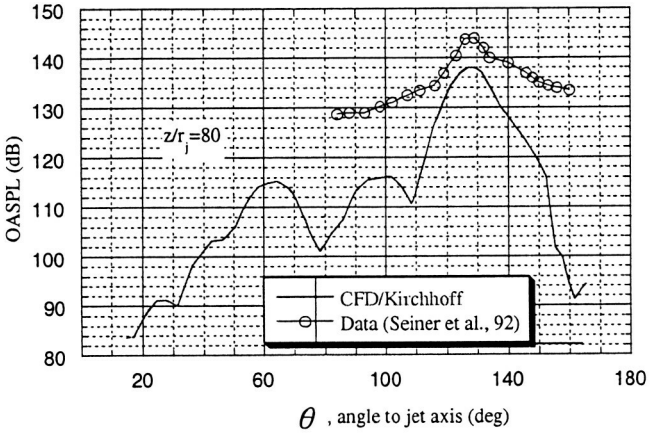

Figure 5b. Comparison of angular OASPL distribution at $z/r_j = 80$

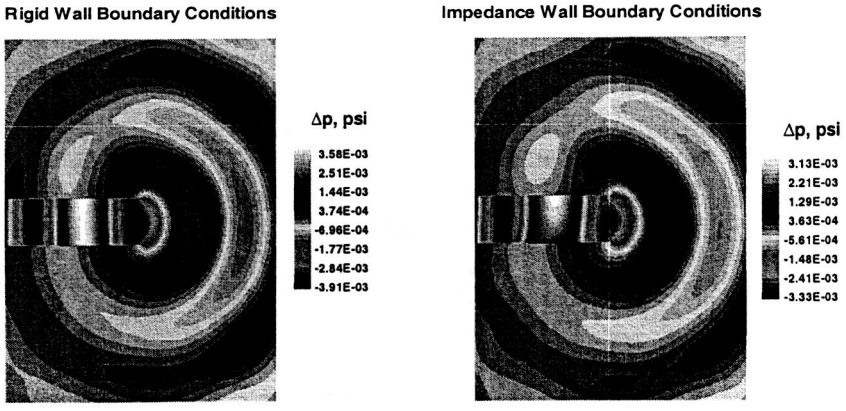

Figure 6a. Instantaneous pressure contours in the duct and its surroundings for the rigid and impedance surface cases ($M_{pk} = 0$, $f = 500\ Hz$)

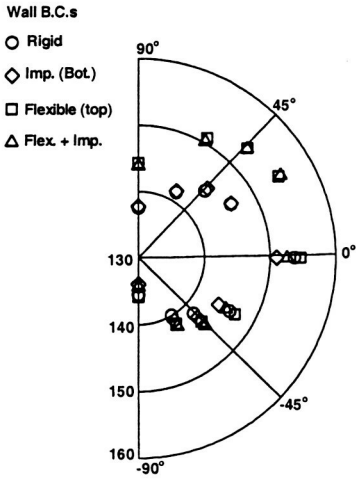

Figure 6b. Farfield directivity for plane wave propagation in a duct with various surfaces at a distance of 2 feet from the exit of the duct (M_{pk}=0)

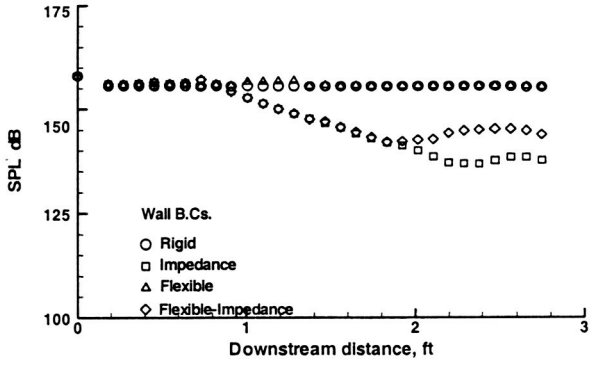

Figure 7. Overall Sound Pressure Level along the top wall of the duct

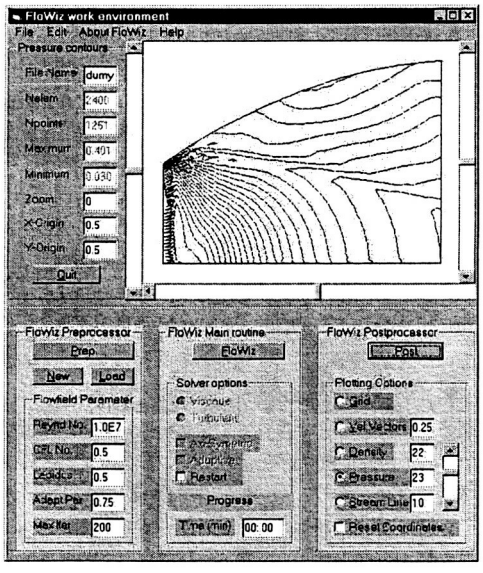

Figure 8. Unified finite-element program

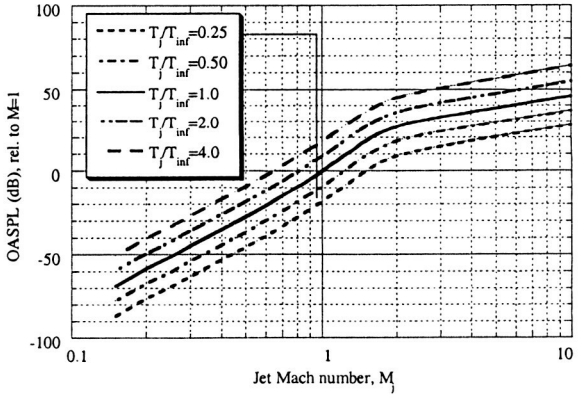

Figure 9. Effect of temperature on overall sound pressure level